Polymer Partitioning from Nonideal Solutions into Protein Voids

Oleg V. Krasilnikov[†] and Sergey M. Bezrukov*[,‡]

Laboratory of Membrane Biophysics, Department of Biophysics and Radiobiology, Federal University of Pernambuco, 50670-901, Recife, PE, Brazil, and Laboratory of Physical and Structural Biology, NICHD, National Institutes of Health, Bethesda, Maryland 20892-0924

Received July 9, 2003; Revised Manuscript Received January 28, 2004

ABSTRACT: Using the change in conductance of a single nanometer-wide protein pore of the α-hemolysin channel to detect pore occupancy by polymers, we measure the equilibrium partitioning of differently sized poly(ethylene glycol)s as a function of polymer concentration in the bulk solution. In the semidilute regime, increased polymer concentration results in a sharp increase in polymer partitioning. Quantifying solution nonideality by osmotic pressure and taking the free energy of polymer confinement by the pore at infinite dilution as an adjustable parameter allows us to describe polymer partitioning only at low polymer concentrations. At larger concentrations the increase in partitioning is much sharper than the model predictions. The nature of this sharp transition between strong exclusion and strong partitioning might be rationalized within the concepts of scaling theory predicting this kind of behavior whenever the correlation length of the monomer density in the semidilute bulk solution becomes smaller than the pore radius. Specific attractive interactions between the protein pore and the polymer that exist in addition to the entropic repulsion accounted for in the present study may also play a role.

Introduction

Understanding polymer partitioning into nanoscale cavities is crucially important in many areas of science and technology. Chromatography is probably the oldest example where the mechanisms of polymer chain distribution between a mobile solution phase and the small voids of a stationary medium underlie the theoretical basis of a number of methods of macromolecule separation.[1] Among more recent examples there is the "osmotic stress technique" , a tool for fundamental studies of inter- and intramolecular forces,[2−4] where accounting for polymer exclusion is essential for data interpretation. Size-dependent partitioning of water-soluble soft polymers has also found its applications in the sizing of aqueous pores of ion channels.[5−10]

Sizing ion channels with polymers is based on the polymer-induced change in channel conductance. Added at the same weight concentration, differently sized polymers reduce bulk solution *conductivity* to a similar extent (e.g., ref 11). However, their action on the channel *conductance* is size-dependent.[12] To enter the pore, large polymers have to overcome a significant entropy barrier. Polymer coils that are much larger than the diameter of the channel aqueous pore influence its conductance only at the pore access areas, introducing relatively small (though measurable[6]) effects. Polymers that are significantly smaller than the pore diameter are able to partition into the pore and inhibit ion currents more efficiently. Therefore, the polymer-induced change in channel conductance quantitatively gauges polymer partitioning.

In our previous studies,[10,13,14] we have shown that the decrease in the poly(ethylene glycol) (PEG) partition coefficient with polymer molecular weight is much sharper than the existing models for polymer partitioning[15−17] predict. This sharp transition is still not understood. It could not be accounted for by the corrections arising from the pore noncylindrical shape or polymer distribution in size.[9,18]

Polymer partitioning was also probed in the reaction of sulfhydryl-directed poly(ethylene glycol)s with the cysteine residues located in the lumen of the α-hemolysin channel[19] and in time-resolved analysis of channel blockage by PEG molecules.[20] Both these studies were performed using diluted PEG solutions and PEG partitioning was found to decrease with the polymer size in satisfactory agreement with the scaling theory[16,17] predictions. The difference between the results of these kinetic studies and the equilibrium partitioning experiments discussed above was attributed to the nonideality of the high concentration polymer solutions used in the equilibrium partitioning measurements.

The problem of solution nonideality in the physics of biological phenomena is quite general. Its realm spreads well beyond channel-facilitated transport. Densely packed molecules of the cell change water activity and, therefore, influence their own functional properties.[4] Moreover, they sterically "crowd" each other[21] inducing intermolecular interactions that are negligible in diluted solutions.

To our knowledge, there are only two theoretical models that give simple analytical results for partitioning of a dilute solution of flexible polymer chains with molecular weight w into a long circular cylindrical pore.[22] The first, "random flight statistics" model[15] accounts for the change in conformational freedom of a polymer modeled as an ideal three-dimensional random walk and is applicable for both weak and strong confinements. The second, scaling model[16,17] deals with strong confinements. For the partition coefficient $p(w)$, which is the ratio of polymer density in the pore to polymer density in the bulk, the scaling model gives a simple exponential form $p(w) = \exp(-w/w_{sc})$, though w_{sc} is not defined within the framework of the scaling

* Corresponding author. Full address: LPSB, NICHD, National Institutes of Health, Bldg. 9, Room 1N-124B, Bethesda, MD 20892-0924. Telephone: 301-402-4701. Fax: 301-496-2172. E-mail: bezrukov@helix.nih.gov.
[†] Federal University of Pernambuco.
[‡] National Institutes of Health.

10.1021/ma030374n CCC: $27.50
Published on Web 03/09/2004

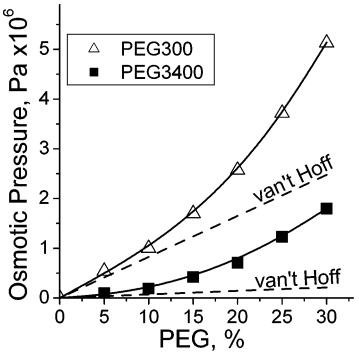

Figure 1. Osmotic pressure of PEG300 and PEG3400 solutions demonstrating significant deviations from the ideal gas behavior and van't Hoff law (interrupted lines). For PEG300 a 2-fold increase due to the polymer−polymer repulsion is seen at concentrations close to 30%, while for PEG3400 it happens already at about 10%. Data are taken (or interpolated) from the osmotic pressure tables at the Brock University website http://aqueous.labs.brocku.ca and fitted by a third-order virial expansion (solid line through PEG300 data) and by a des Cloizeaux approximation (solid line through PEG3400 data).

arguments. Both models refer to dilute polymer solutions and if w_{sc} is properly adjusted, both give quantitatively close predictions (e.g., refs 9 and 10).

We examine the role of polymer solution nonideality by studying partitioning of PEG into the pore of the α-hemolysin channel. We use PEG water solutions at concentrations that correspond to transition from dilute to semidilute regime. Figure 1 shows that at these concentrations the polymer−polymer repulsion is significant and depends on polymer molecular weight. For PEG300 repulsion starts to dominate the solution osmotic pressure at polymer concentrations above 30%. For PEG3400 the nonideality is stronger: it dominates already at about 10% concentration.

Polymer−polymer repulsion is able to increase partitioning dramatically.[22] Indeed, for several PEGs we see a qualitative transition in polymer behavior: with the increasing polymer concentration it changes from practically complete exclusion to practically complete equipartitioning.

We use the osmotic data presented in Figure 1 to rationalize our findings. Chemical potentials of polymer molecules in the bulk and in the pore are calculated as functions of their concentrations following Teraoka et al.[22,23] and using the des Cloizeaux[16] and Ohta and Oono[24] approximations for the osmotic pressure or, alternatively, using an osmotic pressure expansion up to the third-order virial coefficient. We also account for the chain contraction[24] at the increasing polymer concentrations. However, we obtain only qualitative agreement between our experimental results and thermodynamic calculations: high polymer concentrations induce polymer partitioning that is much more pronounced than that deduced from our calculations. We find that the nonideality-induced transition between polymer exclusion and equipartitioning is *much sharper* than the theoretical prediction.

Scaling arguments may offer a qualitative explanation of our findings. According to Daoud and de Gennes,[25] partitioning of long polymers in semidilute solutions is determined by the ratio of the correlation length of monomer density fluctuations to the pore radius. A transition between weak and strong penetration occurs when the polymer concentration is so high that this ratio becomes smaller than one. At these high concentrations confinement does not dominate partitioning any more.

In addition, the polymer partitioning could be modified by the polymer−pore attractive interactions whose existence was established in our previous studies.[13,14] To account for the weak to strong penetration transition, the strength of these interactions per chain would have to increase with the increasing polymer concentration.

Experimental Section

Staphylococcus aureus α-hemolysin (or α-toxin) was a generous gift of Dr. Hagan Bayley of Texas A&M University. Diphytanoylphosphatidylcholine (DPhPC) was purchased from Avanti Polar Lipids (Alabaster, AL), and *n*-pentane was from Burdick and Jackson (Muskegon, MI). Polymeric nonelectrolytes were poly(ethylene glycol)s (PEG) of average molecular weight: PEG200, PEG1500, PEG2000, PEG3400 (Aldrich Chemical Co., Inc., Milwaukee, WI). Other chemicals were analytical grade.

Bilayer lipid membranes were formed at room temperature (23±2 °C) using the lipid monolayer opposition technique from solutions of DPhPC in pentane on a 70 μm diameter aperture in the 15 μm thick Teflon partition as previously described.[10,14] The total capacitance was 90−100 pF, and the film capacitance was close to 40 pF.

Double-distilled water was used to prepare all buffer solutions. Unless stated otherwise, the standard solution used in the bilayer experiments contained 1 M KCl and 5 mM Tris at pH 7.5 adjusted with citric acid. To keep the ion/water molar ratio constant, polymers were added to the standard solution. The conductivity of each solution was measured with a CDM83 (Radiometer Copenhagen) multirange conductivity meter at 23 °C.

The polymer concentration shown on the figures' axes, c %, is the "weight/volume concentration", where c % = 15 means that 100 mL of solution contain 15 g of PEG. This means that the actual dimensionality of these units is 10 kg m^{-3}. In addition to practical convenience of the weight/volume concentration there is a simple relation between c % and polymer molecular concentration c with the dimensionality of m^{-3}: $c = (10 \times c\,\%)/W$, where W is the mass of one polymer molecule in kilograms.

Small amounts of α-hemolysin from a diluted stock solution of 50 μg/mL were added to the cis side of the chamber. The final concentration of the protein in the membrane-bathing solution was about 100 pM. Unless stated otherwise, the experiments were performed at −40 mV of transmembrane voltage. The minus sign means that the potential on the side of protein addition is more negative.

Results and Discussion

The aqueous pore of an ion channel can be regarded as a "nanoscopic cuvette" for studying chemical reactions[26] and polymer−pore interactions.[27−30] In polymer partitioning experiments, because of these interactions and the small size of the pore, it is possible to monitor not only the average occupancies but also the their time variations reflecting characteristic times of particle exchange.[31]

Figure 2 illustrates spontaneous insertions of several α-hemolysin channels into a planar lipid membrane bathed by polymer-free 1 M KCl aqueous solution (panel A) and by the same solution with 20% PEG2000 added (panel B). Polymer addition changes channel behavior in two ways: it reduces channel conductance, and causes vigorous conductance fluctuations seen as an expressed current noise. These fluctuations characterize dynamics of the polymer partitioning[29,31] while the average decrease in conductance reports on a degree of polymer partitioning into the channel pore.

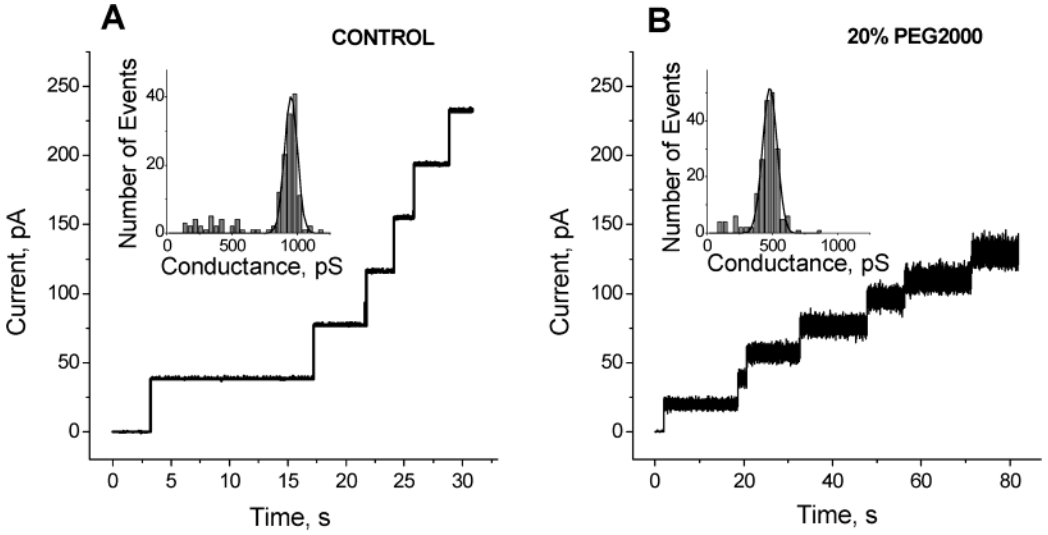

Figure 2. Ion current recordings showing spontaneous insertions of several α-hemolysin channels into the planar lipid membrane in the absence (A) and in the presence (B) of PEG in solution. The membrane was bathed by aqueous solution of 1 M KCl (A) and by the same solution with 20% PEG2000 added (B). Time averaging was 2 ms; transmembrane potential was −40 mV. Amplitude histograms of the single channel conductance measured as 1 s averages are shown in insets. The bin width was 40 pS. More than 200 insertions were analyzed. The normal distribution fits well the main peak of the histograms (solid lines). All other conditions are described in the Experimental Section.

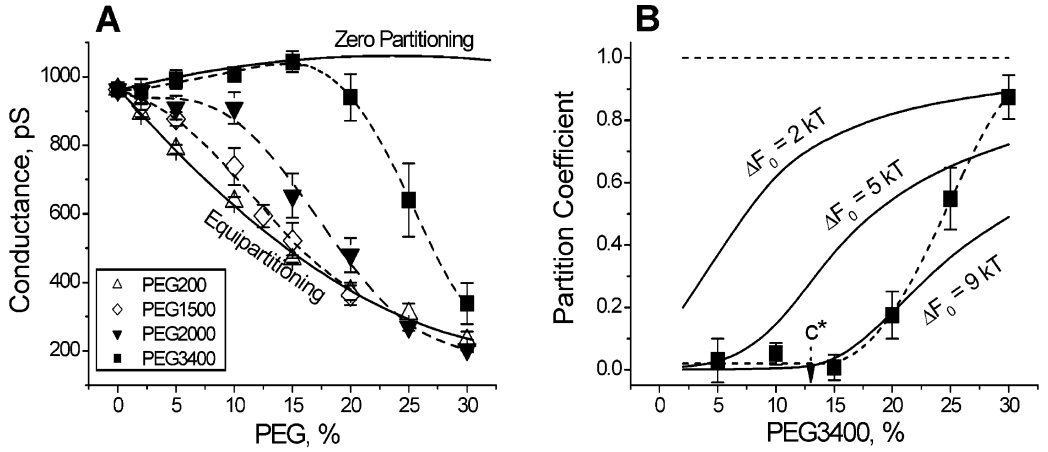

Figure 3. (A) Concentration dependence of channel conductance suggests strong polymer−polymer interactions driving initially differently excluded PEG1500, PEG2000, and PEG3400 into the channel pore. As polymer concentration in the membrane-bathing solution is increased, the three dependences collapse onto the PEG200 curve. The upper solid line shows the channel conductance expected for zero partitioning;[6] the bottom line is drawn through PEG200 data and is assumed to represent polymer equipartitioning. (B) Partition coefficient for PEG3400 (squares) calculated from the conductance change in panel A is shown in comparison with predictions of eq 8 (solid lines). The model predictions, where the free energy of polymer confinement at infinite dilution (ΔF_0) is used as an adjustable parameter, fail to describe the sharp increase in partitioning with polymer concentration. The overlap concentration, c^*, is calculated using the Ohta and Oono approximation for the osmotic pressure in Figure 1 (see text).

Histograms of channel conductances in polymer-free (panel A) and polymer containing (panel B) solutions are shown as Figure 2 insets. To obtain a histogram, a total of 200 spontaneous channel insertions were analyzed. It is seen that the addition of 20% of PEG2000 decreases mean channel conductance by about 50% of its value in polymer-free solution. Each conductance value used for histogram calculation was obtained from the channel current averaged during 1 s. This time is much larger than all characteristic diffusion times in the system[29] including PEG configuration relaxation time. The repeated measurements of conductance of the same channel (not included in histogram) gave results that were reproducible within ±2%. Therefore, the Gaussian-like spread of channel conductances is not related to the accuracy of our measurements (in the presence or absence of PEG) but rather to some minor deviations in the pore structure from channel to channel. Distinctly separate populations of small conductances can be tentatively attributed to contaminations by nicked hemolysin.[32]

Figure 3A summarizes our data on polymer-induced conductance reduction. It demonstrates that the interference of polymers with ionic current and, therefore, polymer partitioning depends on both polymer molecular weight and polymer concentration. The bottom solid curve shows effect of the smallest polymer used, PEG200. As was discussed previously (e.g., refs 13 and 14), due to the PEG−pore attractive interaction, this polymer partitions into the pore even to an excess of its bulk concentration. Addition of PEG200 reduces channel conductance to a slightly higher degree than solution conductivity. Another interesting point is that its effect on channel conductance is indistinguishable from PEG300 effect. These two observations allow us to use the decrease in the channel conductance induced by

PEG200 as a measure of polymer maximum partitioning.

At polymer concentrations smaller than 15%, the largest polymer used in this study, PEG3400, practically does not penetrate into the channel pore at all. In this concentration range, the channel conductance even increases. This is due to the increase in salt activity in the presence of PEG.[6] However, at higher polymer concentrations PEG3400 starts to penetrate the channel and to interfere with the ionic current. At 30% PEG concentration the effect of this large polymer, which is mostly excluded at small concentrations, is very close to the effect of small, easily penetrating PEG200.

To derive the partition coefficient from the conductance vs concentration data in Figure 3A, we use our usual assumption that the polymer-induced reduction in channel conductance is proportional to polymer partition coefficient.[13] If we also assume that partition coefficient for PEG200 equals one, we have

$$p(c\,\%, w) = \Delta g(c\,\%, w)/(g_{max}(c\,\%) - g_{min}(c\,\%)) \quad (1)$$

where $\Delta g(c\,\%, w)$ is the conductance reduction caused by PEG with molecular weight w in comparison to $g_{max}(c\%)$, which is the channel conductance in the presence of completely excluded polymers; $g_{min}(c\%)$ is the channel conductance in the presence of completely penetrating small polymers (PEG200). The zero partitioning curve in Figure 3A represents $g_{max}(c\,\%)$ and is calculated as described in ref 6. It accounts for the following two effects of PEG addition: (i) an increase in salt activity that increases conductance of the channel proper and (ii) a decrease in bulk solution conductivity that decreases conductance of the channel contacts with the bulk.

The results for PEG3400 are plotted in Figure 3B. Increased concentration drives this polymer into the channel pore. Nearly completely excluded at concentrations smaller than 15%, PEG3400 starts to penetrate the pore at higher concentrations with partition coefficient approaching unity at 30% concentration.

Solution Nonideality. An increase in partition coefficient at increasing polymer concentration can be thought of as a manifestation of polymer−polymer repulsion that drives polymers into the pore to an excess of simple proportionality between their pore and bulk concentrations.

To quantify the effects of solution nonideality we use osmotic pressure of PEG-containing solutions. First, for the nonideal part of the pressure, we consider des Cloizeaux approximation[16] that was recently shown to adequately describe PEG data:[33]

$$\Delta\Pi_{osm}(\phi) = \alpha(kT/a^3)\phi^{9/4} \quad (2)$$

where k and T have their usual meanings of the Boltzmann constant and the absolute temperature, a is the "persistence length" , α is a constant on the order of unity, and ϕ is the monomer volume fraction. Introducing β by $\beta c^{9/4} = \phi^{9/4}$ we relate the monomer volume fraction to polymer concentration c. Because of about a 10% difference in partial specific volumes of water and PEG, β is slightly concentration-dependent; we neglect this dependence and take its value for infinite dilutions. Then, for the reduced form of osmotic pressure, $P(c)$, we can write:

$$P(c) \equiv \frac{\Pi_{osm}(c)}{ckT} = 1 + \alpha\beta(1/a^3)c^{5/4} \quad (3)$$

For the chemical potential of polymer in the bulk,[22,23] we have

$$\mu_b = \mu_0 + kT \ln c_b + kTI(c_b) \quad (4)$$

where c_b is the bulk polymer concentration and the nonideality term is

$$I(c_b) = P(c_b) - 1 + \int_0^{c_b} \frac{P(c) - 1}{c}\,dc \quad (5)$$

Calculating this term in the des Cloizeaux approximation (eq 3), we arrive at

$$\mu_b = \mu_0 + kT \ln c_b + \frac{9}{5}\alpha\beta(kT/a^3){c_b}^{5/4} \quad (6)$$

Following Teraoka et al.,[22,23] we write the chemical potential of the polymer in the pore in the same form as in the bulk but offset by the concentration-dependent free energy of polymer confinement, $\Delta F(c_b)$

$$\mu_p = \mu_0 + kT \ln c_p + \frac{9}{5}\alpha\beta(kT/a^3){c_p}^{5/4} + \Delta F(c_b) \quad (7)$$

This assumption is indeed a gross simplification of the actual situation. For example, we neglect polymer−pore interactions other than purely entropic and disregard possible modifications of polymer−polymer interactions within the pore due the changes in the properties of water confined by protein cavities.[34] However, this idealized approach permits us to get a quantitative "gauge" for the experimental results.

Equating the polymer's chemical potentials in the bulk and in the pore, we obtain

$$kT \ln p = \frac{9}{5}\alpha\beta(kT/a^3){c_b}^{5/4}(1 - p^{5/4}) - \Delta F(c_b) \quad (8)$$

where the partition coefficient is defined as a ratio of polymer concentrations in the pore and in the bulk $p \equiv c_p/c_b$.

For the free energy of chain confinement by the pore, we write

$$\Delta F(c_b) = \Delta F_0\left(\frac{R_F(c_b)}{R_F(0)}\right)^{5/3} \quad (9)$$

where $R_F(c_b)$ is the concentration-dependent end-to-end distance for which we use an approximation given by Ohta and Oono.[24] The numerical coefficient $\alpha\beta(kT/a^3)$ can be obtained from fitting eq 3 to the osmotic pressure data in Figure 1 thus leaving the only adjustable parameter in eq 8, the free energy of polymer confinement at infinite dilution, ΔF_0.

Comparison of eq 8 predictions with experiment is presented in Figure 3B. The experimental data show much sharper dependence on polymer concentration than the theoretical curves. By decreasing ΔF_0, we are able to achieve a better fit at high polymer concentrations, but only at the expense of losing the fit at low concentrations. In agreement with Teraoka et al.[23] we find that the effect of chain contraction at the increasing polymer concentration is small; the leading cause of nonlinear partitioning is the nonideality in osmotic

pressure. The buildup in osmotic pressure (Figure 1) drives polymer chains into the pore to an excess of the simple linear partitioning.

Very close theoretical predictions were obtained using the osmotic pressure approximation derived by Ohta and Oono[24] according to which

$$P(X) = 1 + \frac{1}{2}X \exp\left\{\frac{1}{4}\left[\frac{1}{X} + \left(1 - \frac{1}{X^2}\right)\ln(1 + X)\right]\right\} \quad (10)$$

where X is the reduced concentration that is defined through the overlap concentration c^*as $X \cong 3.49c/c^*$. Fitting eq 10 to the data in Figure 1 and using this expression to calculate the nonideality term in eq 4, we arrive at the theoretical curves that practically coincide with the solid lines in Figure 3B. Qualitatively similar results have also been found using the third-order virial expansion (not shown). The measured dependence of polymer partitioning is much steeper than the theoretical predictions that use osmotic pressure data in Figure 1 to quantify polymer−polymer interactions.

The overlap concentration obtained by fitting eq 10 to the PEG3400 data in Figure 1 is 12.9% which corresponds to $c^* = 2.28 \times 10^{25}$ m^{-3}. Using des Cloizeaux definition of the overlap concentration[35] $c^* = 1/(\sqrt{2}\, R_g^{(0)})^3$, for the radius of gyration at infinite dilution we have $R_g^{(0)} = 24.9$ Å. Consequently, for the end-to-end distance, which is related to the gyration radius by[23] $R_F/R_g = 2.51$, we obtain $R_F = 62.5$ Å. The hydrodynamic radius of PEG3400 can be found from[23] $R_H/R_g = 0.64$ as $R_H = 15.9$ Å. This value is in good agreement with the experimental data.[8,36] All these numbers should be compared to the effective radius of the α-hemolysin pore which is close to 10 Å.[10,14,37]

The sharp transition between the weak and strong partitioning in Figure 3B is observed at polymer concentrations just above c^*, the overlap concentration of 12.9%. Qualitatively, this behavior is in perfect agreement with the scaling analysis by Daoud and de Gennes[25] who predicted that partitioning in the semidilute solutions is governed by the correlation length of monomer density fluctuations in the bulk solution, ξ_b, and not by the characteristic size of a polymer molecule. With the increasing polymer concentration the weak-to-strong partitioning transition occurs when the decreasing correlation length becomes smaller than the pore aperture.

Unfortunately, the scaling analysis by Daoud and de Gennes[25] does not give analytical results for the most interesting regime, where bulk polymer concentration exceeds c^*, but is still smaller than the concentration corresponding to the strong partitioning (concentration range 15−25% in our experiments with PEG3400). For this reason, a quantitative comparison with our results is rather difficult. Scaling calculations of the partition coefficient for the confinement in a pore in this regime are underway.[50]

To our knowledge, the transition between weak and strong partitioning at the increasing polymer concentration was observed in light-scattering experiments by several groups (e.g., see ref 22 for a review). However, the quantitative analysis of the partitioning was quite satisfactory within the framework of the nonideality model described above.[23] Figure 3B demonstrates that the sharp transition obtained in the present study cannot be rationalized by this model. A similar behavior was recently found for a model system in Monte Carlo simulations of polymer partitioning into a square channel.[38]

Quality of Polymer Samples. In our analysis, we treat polymers as objects composed of molecules of exactly equal size, identified by their nominal molecular weight. In reality, PEG samples are always represented by finite distributions of molecular weights so that the nominal weight given by the manufacturer is, at best, the average weight. What are the possible effects of these distributions in polymer partitioning experiments?

As was discussed elsewhere for experiments where the molecular weight was varied but monomer concentration was kept constant,[9,18] the presence of higher- or lower-weight fractions only broadens the transition between penetration and exclusion. Indeed, suppose that each polymer sample is a mixture of two differently sized polymers, represented by their average molecular weight. Then, in the set of experiments where the average weight is increased, the exclusion should start sooner (higher-weight fractions start to be excluded first) and should end later (lower-weight fractions stop penetrating last). The resulting dependence of partition coefficient on the polymer molecular weight would be "smeared" by the samples' finite weight distributions.

Here we describe experiments with the conserved molecular weight, but increasing monomer concentration. One may think that the lower-weight polymer fractions (e.g., to be radical, PEG200 in the "PEG3400" sample) progressively partition into the channel pore driven there by the increasing pressure produced by the higher-weight fraction. First, we checked this conjecture theoretically by complementing eq 8 with an additional similar equation for the lower-weight fraction and solving the two equations together numerically. As a result, depending on the relative amount of the second fraction and its relative molecular weight, we could observe significant corrections to the theoretical curves (data not shown). The lower-weight fraction does enter the pore progressively with the total polymer concentration; however, the effect can be well described by choosing smaller values of ΔF_0 in eqs 8 and 9 without sharpening the concentration dependence (see also ref 39). Second, to characterize sample quality we used gel permeation chromatography and determined the number-average (M_n) and weight-average (M_w) molecular masses of our PEG samples. The ratio M_w/M_n was found to be close to unity, though increasing with the polymer molecular weight. In particular, it was equal 1.08 for PEG400 and 1.18 for PEG4600.

Effects of Osmotic Stress. Conventional interpretation of osmotic stress effects on a protein molecule is that osmotic pressure changes equilibrium between different conformational states of the molecule.[4] For ion channels, different states are often seen as different levels of the channel conductance whose probabilities change in the presence of osmolytes.[3,40,41]

We found that addition of nonpenetrating polymers to membrane-bathing solutions resulted in a decrease of the α-hemolysin channel dwell time in the open conformation (data not shown). To obtain the conductance data reported here we selected only fully open states of the channel. However, there is a hypothetical possibility that channel conductance is reduced by the change in channel dimensions due to finite protein elasticity.[42] For osmotic pressures of about 2×10^6 Nm^{-2} corresponding to 30% concentration of PEG3400, the

force applied to a channel wall of 1 nm^2 area can be estimated as 2 pN. This force is to be compared with a characteristic force that a single charge is experiencing in a typical transmembrane field. Taking potential difference of 100 mV acting across a 5 nm thick membrane we obtain 3 pN. Thus, the "osmotic force" of excluded PEG at 30% bulk polymer concentration is comparable with a typical electric force per membrane protein charge.

Being a plausible candidate, the idea of the osmotically induced change in the pore dimensions as the reason for the observed conductance reduction at high polymer concentrations contradicts the data in Figure 3A. Indeed, PEG200, which easily penetrates the channel, is not supposed to exert pore-collapsing osmotic stress at all. Larger PEG1500, PEG2000, and PEG3400 should produce different osmotic stress because they are excluded to a different degree.[40,41] However, their effects on channel conductance practically coincide with that of PEG200 at high polymer concentrations. This observation strongly suggests that the mechanism of conductance reduction is common to both small, freely penetrating polymers, which do not exert the osmotic force on the channel wall, and large, completely excluded polymers. Therefore, we conclude that the channel conductance reduction in the presence of either small or large polymers is not caused by channel elastic deformation by osmotic stress.

Finally, addition of polymers into the membrane-bathing solution may influence the natural distribution of channel sizes (Figure 2A, inset) by some kind of osmotically driven "pre-selection" . Indeed, it could be imagined that osmotic stress shifts the conformational distribution of channels in favor of conformations with smaller volumes of polymer-inaccessible water and, therefore, with smaller conductances. This effect would be manifested as an extra decrease in the average channel conductance in the presence of poorly penetrating PEGs.

To explore this possibility, we performed a series of measurements where the effect of changing polymer concentration on channel conductance was studied on the same single channel. Figure 4 illustrates one of these experiments. Here, the protocol is different from that of Figure 2 and all other experiments in this study. Instead of reconstituting channels at the final PEG3400 concentration of 30%, we first reconstituted the channel at 15% PEG3400 concentration that corresponds to exclusion (squares in Figure 3), recorded its conductance, and only then increased polymer concentration to 30%. The denser 30% PEG3400 solution was slowly added to the bottom of the membrane cell until the solution level went above the membrane aperture. Absence of significant mixing between the initial and final solution was verified by the use of a dye in the denser solution and, independently, by the index of refraction measurements of PEG concentration in the cell. It is seen that the action of the denser solution is delayed by several minutes reflecting the rate of the denser solution exchange with the initial solution at the membrane surface. After the delay, the channel conductance stabilizes at a new level that is in good agreement with the data in Figure 3A. Thus, these control experiments demonstrate that the effect of the possible osmotic "pre-selection" discussed above is negligible.

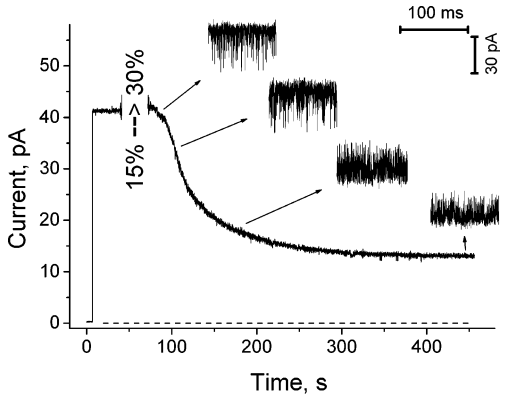

Figure 4. Monitoring changes in conductance of the same single channel at the increased polymer concentration. After channel insertion into the membrane (the leftmost part of the recording), the initial solution of 15% PEG3400 was substituted by solution containing 30% PEG3400. Transmembrane potential was −40 mV. The data are presented at 100 ms averaging. The dashed line indicates zero current. Insets: samples of 100 ms duration taken from different parts of the recording marked by arrows are shown at 0.1 ms resolution. It is seen that the channel is mostly in its high-conductance state, that is, the mostly polymer-free at 15% and is mostly occupied by polymer at 30% PEG concentration.

Effects of the Electric Field. We discuss our main findings in terms of equilibrium polymer partitioning, and our measurements are performed at a relatively small transmembrane voltage of 40 mV. Nevertheless, due to the small length of the channel (10 nm), the electric field created by this voltage in the channel is rather strong (40 mV/10 nm = 4×10^6 V/m; it is even higher in certain parts of the channel if one accounts for the channel irregular geometry). This field strength may be enough to distort the channel/polymer equilibrium due to polarization effects and the well-known ability of PEG to bind cations in electrolyte water solutions.[8,43]

To test this hypothesis, we measured polymer partitioning at equilibrium conditions. We made use of the main idea of the fluctuation−dissipation theorem that equilibrium fluctuations can be related to the system impedance. In the case of current fluctuations the corresponding relation takes the form of the Nyquist formula[44]

$$S_I(f) = 4kT\ \mathrm{Re}(1/Z(f)) \qquad (11)$$

where $S_I(f)$ is the equilibrium power spectral density of current fluctuations and $Z(f)$ is system's impedance at frequency f. At low frequencies, where we can neglect the frequency dispersion in channel ionic conductance G we have $1/Z(f) \cong G$. Therefore, we can calculate system conductance from system noise without application of any transmembrane potential

$$G = S_I(0)/4kT \qquad (12)$$

Results of such an experiment are shown in Figure 5. All three spectra were measured at *zero applied potential* with the amplifier kept in the "voltage clamp" mode. To be sure that a possible misbalance in electrode potentials did not interfere with the measurement, it was the current though the channels that was minimized to a level smaller than 0.1 pA. The upper spectrum in Figure 5A was measured from 13 channels

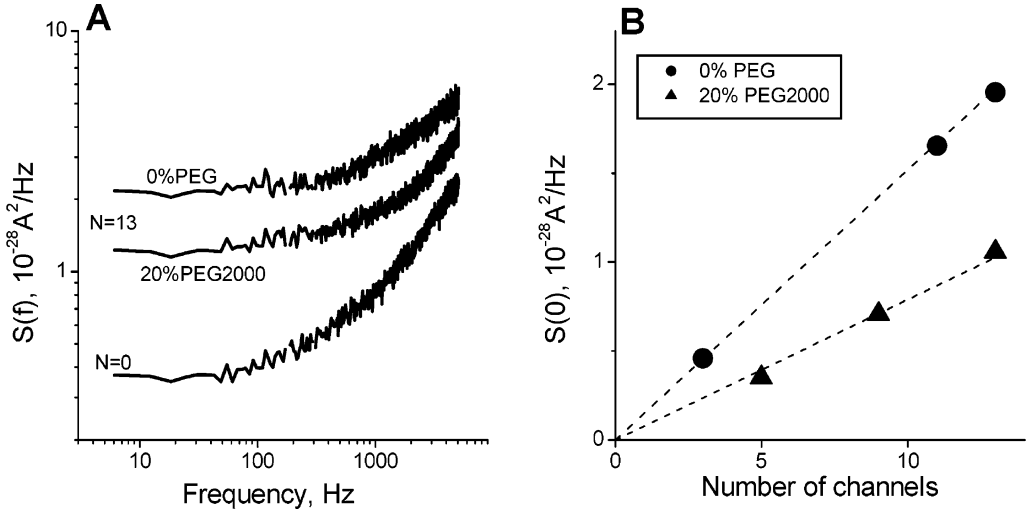

Figure 5. Making use of the fluctuation−dissipation theorem to measure channel conductance at equilibrium. (A) Spectra of equilibrium current fluctuations at zero transmembrane potential report on the membrane conductance. Equilibrium noise of 13 channels ($N = 13$) significantly exceeds background noise ($N = 0$) and is decreased by polymer addition. The rising parts of the spectra are mostly related to the finite electrode resistance, amplifier noise, and membrane capacitance.[49] (B) Equilibrium channel noise, averaged over the first decade of the frequency range with the background subtracted, as a function of the number of channels. Addition of 20% PEG2000 decreases the noise by ~1.8 times.

in the membrane in the absence of PEG, so that this corresponded to voltage misbalance smaller than 0.1 pA/(13 × 0.95 nS), which is 8 μV. The background spectrum was taken before protein addition; it represents a membrane without channels, though most of the low-frequency noise originates from the amplifier feedback resistor ("whole-cell" mode, Axopatch 200B, Axon Instruments, Inc., Foster City, CA).

Insertion of channels increases both membrane conductance and, in agreement with eq 11 predictions, ionic current noise (upper curve). Addition of polymers reduces channel conductance and its equilibrium noise (middle curve). Noise intensities were obtained from these spectra by averaging over the frequency band 7−100 Hz with the background subtracted. They are shown in Figure 5B as functions of the number of channels. It is seen that equilibrium noise increases with the number of channels in both solutions, but in PEG-free solution it grows in larger increments. For polymer-free solutions it is $(1.5 \pm 0.1) \times 10^{-29}$ A^2/Hz per channel, and for 20% PEG2000 it is $(0.83 \pm 0.07) \times 10^{-29}$ A^2/Hz per channel. Using eq 12 we obtain 0.93 ± 0.06 and 0.51 ± 0.04 nS, correspondingly. These numbers should be compared with 0.96 ± 0.02 and 0.48 ± 0.05 nS obtained from the $I-V$ relationship at −40 mV. On the basis of these results, we conclude that the partitioning we discuss here is an equilibrium phenomenon.

Conductance Reduction as a Measure of Polymer Partitioning. We deduce polymer partitioning coefficient from the polymer-induced reduction in channel conductance. Our usual assumption is the linear relation between partition coefficient and conductance change, eq 1. This assumption is based on PEG effect on electrolyte solution conductivity (e.g., Figure 1 in ref 11) showing that in the concentration range 0−15%, the relative deviation from a linear regression does not exceed 0.03 for any point.

For the higher polymer concentrations used in the present study this deviation is larger.[11] Nonlinearity between the change in channel conductance and average polymer concentration in the channel pore could introduce significant corrections. To account for this nonlinearity we use the relative change in channel conductance in the presence of small, easily penetrating PEG200 (bottom curve in Figure 3A). Taking this approximation to refine our calculation of the partition coefficient, we obtain only small corrections (not shown). The difference between the linear and the refined approximation is small enough not to change any of our conclusions.

Importantly, all three dependences for partially excluded PEG1500, PEG2000, and PEG3400 collapse onto equipartitioning curve (Figure 3A) so that the effect becomes independent of polymer molecular weight. This finding strongly suggests that at high concentrations the mechanism of channel conductance reduction by these polymers is the same as for the freely partitioning PEG200. Similar to the molecular-weight-independent effect of PEG addition on the bulk solution conductivity,[11] the reduction is due to the dilution of ion concentration and to the increase in solution microviscosity by the polymers in the channel pore.

Conclusions

Here we have studied how polymer partitioning depends on the polymer concentration. As is reasonable to expect, higher polymer concentrations correspond to higher partitioning. However, we find that the transition between exclusion and penetration at the varying polymer concentration is sharper than predicted by theories that account only for polymer solution nonideality and concentration-dependent entropic repulsion between the polymer and the pore. Thus, our findings differ from those of the previously reported nonlinear polymer partitioning experiments (e.g., ref 23), where the main results could be quantitatively explained by the polymer−polymer repulsion derived from the osmotic pressure data.

Recent Monte Carlo simulations of polymers in a slit[45,46] and, in particular, a square channel[38] in contact with a reservoir demonstrated a highly nonlinear partitioning in semidilute solutions. Importantly, in agreement with earlier predictions[25] it was concluded[38] that it is not the chain length but the correlation length of

monomer density fluctuations in the exterior solution that governs the partitioning in semidilute solutions. These results may be crucially important for understanding polymer partitioning into protein voids studied here.

One of the steps of future theoretical effort could also be to account for the polymer−pore attractive interactions, existence of which was revealed in our previous studies.[13,14] It is quite obvious that attractive interactions between polymer chain segments and the pore walls increase polymer partitioning by partially compensating entropic repulsion.[47] Moreover, if the strength of these interactions is assumed to grow with the polymer concentration in the pore, one should expect a sharpening of the transition between exclusion and penetration.

Other essential modifications of the model could be related to the finiteness of channel dimensions. Indeed, the polymer length is larger not only than the pore radius of 1 nm but also the pore length (e.g., the length of a fully extended PEG3400 molecule is close to 30 nm, while the channel length is 10 nm). Therefore, partial polymer confinement[48] may be of importance.

Acknowledgment. We are grateful to Adrian Parsegian, Per Hansen, Sasha Berezhkovskii, and Don Rau for fruitful discussions and comments on our manuscript.

References and Notes

(1) Giddings, J. C. *Unified Separation Science;* John Wiley: New York, 1991.
(2) Parsegian, V. A.; Rand, R. P.; Fuller, N. L.; Rau, D. C. *Methods Enzymol.* **1986**, *127*, 400−416.
(3) Zimmerberg, J.; Parsegian, V. A. *Nature (London)* **1986**, *323*, 36−39.
(4) Parsegian, V. A.; Rand, R. P.; Rau, D. C. *Proc. Natl. Acad. Sci. U.S.A.* **2000**, *97*, 3987−3992.
(5) Krasilnikov, O. V.; Sabirov, R. Z.; Ternovsky, V. I.; Merzliak, P. G.; Muratkhodjaev, J. N. *FEMS Microbio. Immunol.* **1992**, *105*, 93−100.
(6) Bezrukov, S. M.; Vodyanoy, I. *Biophys. J.* **1993**, *64*, 16−25.
(7) Krasilnikov, O. V.; Da Cruz, J. B.; Yuldasheva, L. N.; Varanga, W. A.; Nogueira, R. A. *J. Membr. Biol.* **1998**, *161*, 83−92.
(8) Krasilinikov, O. V. In *Structure and Dynamics of Confined Polymers*; Kasianowicz, J. J., Kellermayer, M. S. Z., Deamer, D. W., Eds.; Kluwer Publishers: Dordrecht, The Netherlands, 2002; pp 97−115.
(9) Bezrukov, S. M.; Kasianowicz, J. J. In *Structure and Dynamics of Confined Polymers*; Kasianowicz, J. J., Kellermayer, M. S. Z., Deamer, D. W., Eds.; Kluwer Publishers: Dordrecht, The Netherlands, 2002; pp 117−130.
(10) Rostovtseva, T. K.; Nestorovich, E. M.; Bezrukov, S. M. *Biophys. J.* **2002**, *82*, 160−169.
(11) Stojilkovic, K. S.; Berezhkovskii, A. M.; Zitserman, V. Yu.; Bezrukov, S. M. *J. Chem. Phys.* **2003**, *119*, 6973−6978.
(12) Krasilnikov, O. V.; Sabirov, R. Z.; Ternovsky, V. I.; Merzlyak, P. G.; Tashmukhamedov, B. A. *Gen. Physiol. Biophys.* **1988**, *7*, 467−473.
(13) Bezrukov, S. M.; Vodyanoy, I.; Brutyan, R. A.; Kasianowicz, J. J. *Macromolecules* **1996**, *29*, 8517−8522.
(14) Merzlyak, P. G.; Yuldasheva, L. N.; Rodrigues, C. G.; Carneiro, C. M. M.; Krasilnikov, O. V.; Bezrukov, S. M. *Biophys. J.* **1999**, *77*, 3023−3033.
(15) Casassa, E. F. *Polymer Lett.* **1967**, *5*, 773−778.
(16) de Gennes, P.-G. *Scaling Concepts in Polymer Physics*; Cornell University Press: Ithaca, NY, 1979.
(17) Grosberg, A. Yu.; Khokhlov, A. R. *Statistical Physics of Macromolecules*; AIP Press: New York, 1994.
(18) Bezrukov, S. M.; Kasianowicz, J. J. *Biol. Membr.* **2001**, *18*, 453−457.
(19) Movileanu, L.; Bayley, H. *Proc. Natl. Acad. Sci. U.S.A.* **2001**, *98*, 10137−10141.
(20) Movileanu, L.; Cheley, S.; Bayley, H. *Biophys. J.* **2003**, *85*, 897−910.
(21) Minton, A. P. *Methods Enzymol.* **1998**, *295*, 127−149.
(22) Teraoka, I. *Prog. Polym. Sci.* **1996**, *21*, 98−149.
(23) Teraoka, I.; Langley, K. H.; Karasz, F. E. *Macromolecules* **1993**, *26*, 287−297.
(24) Ohta, T.; Oono, Y. *Phys. Lett.* **1982**, *89A*, 460−464.
(25) Daoud, M.; de Gennes, P. G. *J. Phys. (Paris),* **1977**, *38*, 85−93.
(26) Bezrukov, S. M.; Kasianowicz, J. J. *Phys. Rev. Lett.* **1993**, *70*, 2352−2355.
(27) Kasianowicz, J. J.; Brandin, E.; Branton, D.; Deamer, D. W. *Proc. Natl. Acad. Sci. U.S.A.* **1996**, *93***,** 13770−13773.
(28) Bayley, H.; Martin, C. R. *Chem. Reviews* **2000**, *100*, 2575−2594.
(29) Bezrukov, S. M. *J. Membr. Biol.* **2000**, *174*, 1−13.
(30) Kong, C. Y.; Muthukumar, M. *Electrophoresis* **2002**, *23*, 2697−2703.
(31) Bezrukov, S. M.; Vodyanoy, I.; Parsegian, V. A. *Nature (London)* **1994**, *370*, 279−281.
(32) Krasilnikov, O. V.; Merzlyak, P. G.; Yuldasheva, L. N.; Azimova, R. K.; Nogueira R. A. *Med. Microbiol. Immunol.* **1997**, *186*, 53−61.
(33) Hansen, P. L.; Cohen, J. A.; Podgornik, R.; Parsegian, V. A. *Biophys. J.* **2003**, *84*, 350−355.
(34) Yu, B.; Blaber, M.; Gronenborn, A. M.; Clore, G. M.; Caspar, D. L. D. *Proc. Natl. Acad. Sci. U.S.A.* **1999**, *96*, 103−108.
(35) des Cloizeaux, J.; Jannink, G. *Polymers in Solution: Their Modeling and Structure*; Clarendon Press: Oxford, England, 1990.
(36) Kuga, S. *J. Chromatogr.* **1981**, *206*, 449−461.
(37) Song, L.; Hobaugh, M. R.; Shustak, C.; Cheley, S.; Bayley, H.; Gouaux, J. E. *Science* **1996**, *274*, 1859−1866.
(38) Cifra, P.; Teraoka, I. *Polymer* **2002**, *43*, 2409−2415.
(39) Teraoka, I.; Zhou, Z.; Langley, K. H.; Karasz, F. E. *Macromolecules* **1993**, *26*, 3223−3226.
(40) Vodyanoy, I.; Bezrukov, S. M.; Parsegian, V. A. *Biophys. J.* **1993**, *65*, 2097−2105.
(41) Parsegian, V. A.; Bezrukov, S. M.; Vodyanoy, I. *Biosci. Rep.* **1995**, *15*, 503−514.
(42) Zaccai, G. *Science* **2000**, *288*, 1604−1607.
(43) Harris, J. M. In *Poly(Ethylene Glycol) Chemistry. Biotechnical and Biomedical Applications;* Harris, J. M., Ed.; Plenum Press: New York, 1992; pp 1−14.
(44) Nyquist, H. *Phys. Rev.* **1928**, *32*, 110−113.
(45) Cifra, P.; Bleha, T. *Macromolecules* **2001**, *34*, 605−613.
(46) Bleha, T.; Cifra, P. *Polymer* **2003**, *44*, 3745−3752.
(47) Davidson, M. G.; Suter, U. W.; Deen, W. M. *Macromolecules* **1987**, *20*, 1146−1152.
(48) Hermsen, G. F., de Geeter, B. A., van der Vegt, N. F. A.; Wessling, M. *Macromolecules* **2002**, *35*, 5267−5272.
(49) Sigworth, F. J. In *Single-Channel Recording*, 2nd ed.; Sakmann, B.,Neher, E., Eds.; Plenum Press: New York, 1995; pp 95−127.
(50) Shusharina, N. P.; Rubinstein, M. Private communication.

MA030374N